博 士 論 文

Near-infrared light-boosted antimicrobial activity of minocycline/hyaluronan/carbon nanohorn composite toward peri-implantitis treatments
(インプラント周囲炎治療を目的とした近赤外光応答性ミノサイクリン／ヒアルロン酸／カーボンナノホーン複合体の抗菌効果の検討)

令和７年３月申請

北海道大学
大学院歯学院口腔医学専攻

小　西　大　輔

Introduction

Dental implants constitute a widely used treatment for the replacement of missing teeth[1,2]. With the increasing prevalence of dental implants, peri-implantitis has emerged as a serious complication[3,4], posing a significant challenge to the success of implant procedures. Peri-implantitis has been estimated to occur in 10.7–47.2% of dental implant patients within 10 years following implant placement[5,6]. Most commonly, peri-implantitis is caused by adherence (to the implant surface) of oral bacteria[7], typically consisting of *Aggregatibacter actinomycetemcomitans* (*A.a.*)[8,9].

Currently, a variety of approaches are employed for the treatment of peri-implantitis, including air-polishing devices, erbium-doped yttrium aluminum garnet (Er:YAG) lasers, ultrasound devices, and surgical therapy[10]. However, implant surfaces typically are modified to promote osseointegration[11]; the resulting three-dimensional complex surface structures make the removal of bacteria from these matrices difficult. Local administration of antibiotics, such as minocycline (MC), also is used to treat peri-implantitis. However, the complexity of the implant surface structures and the depth of pockets pose challenges for drug delivery to the affected areas[12–14]. Moreover, single local administration of antibiotics necessarily provides only a temporary effect, and maintenance of antibiotics and their effects at the affected area remains difficult. Furthermore, the use of antibiotics comes with drawbacks, including the potential for the induction of allergic reactions and/or bacterial resistance[15,16], and the consumption of such antibacterials is increasingly a public health concern. These problems render the treatment of peri-implantitis challenging. To address these issues, the development of drug delivery systems (DDSs) that are effective against peri-implantitis is urgently needed.

Near-infrared (NIR) light, particularly in the 700- to 1300-nm range (considered the biological window[17,18]), is known to exhibit high tissue penetration[19] without incurring damage[17]. NIR light penetrates up to one centimeter in mucosal tissue[19]. Goaslind et al. reported that the thickness of the free gingiva is typically 1.56 ± 0.39 mm (mean ± SD), while that of the attached gingiva is typically 1.25 ± 0.42 mm, with a mean total thickness of 1.41 mm[20]. Therefore, NIR light is expected to readily reach implant surfaces through the peri-implant mucosa. Taking advantage of these characteristics of NIR light, there have been several reports on the use of NIR light for the treatment of peri-implantitis. For example, photodynamic therapy is used to remove bacteria, all but one example (to the best of our knowledge) employed indocyanine green (ICG) in combination with an NIR laser.The sole exception is our report employing carbon nanohorns (CNHs)[21]. As we demonstrated in that work, our CNH-based system demonstrates superior photostability compared to ICG, given that the latter decomposes during prolonged illumination[19].

Carbon nanomaterials such as carbon nanotubes and graphene have been investigated as carriers for DDSs in combination with NIR light[22,23]. In addition to those carbon nanomaterials, CNHs have garnered significant attention for biomedical applications, due in part to the unique structure of the nanohorns. CNH are composed of horn-shaped tips that are 2-5 nm in diameter and 40-50 nm in length. These tubules assemble to

form spherical aggregates with diameters of approximately 100 nm[24]. Notably, CNHs are known to be highly biocompatibile, given the absence of metal catalysts in their preparation and their approximately isotropic nature in three dimensions, which may contribute to their low toxicity. Indeed, preclinical evaluations have shown that CNHs exhibit only minimal toxicity[25]. The unique properties of these structures make CNHs promising matrices for various biomedical applications. In previous work, we reported potential applications of CNH-modified titanium oxide for use in dental implants; surfaces coated with CNHs were shown to promote osseointegration[26,27]. CNHs have been found to effectively encapsulate drugs and biomolecules, making these structures attractive for targeted DDSs. Given that CNHs exhibit such distinctive characteristics, research has explored the application of these compounds in DDSs[28–30]. However, to our knowledge, CNHs have only rarely been examined for use in antibiotic-targeted DDSs, especially for peri-implantitis. Minocycline (MC) is one of the antibiotics used for peri-implantitis[31] and exhibits bacteriostatic activity[32]. Our previous study reported that MC-loaded CNHs (MC/CNHs) have antibacterial effects[33]. Therefore, we attempted to control the release of MC by further irradiation with NIR. However, MC was not released by NIR irradiation because it was tightly bound to CNHs.

To overcome this limitation, we employed, in the present study, an approach in which hyaluronan [hyaluronic acid (HA)] is bound to CNHs and loaded with MC; we conjectured that the MC in the resulting material would exhibit enhanced antibacterial activity. Notably, upon irradiation, CNHs experience a rapid temperature increase due to photothermal conversion, enabling the CNHs to reach temperatures suitable for inducing various thermal effects that may be exploited for several applications, including photothermal therapy and controlled drug release[34,35]. Specifically, NIR irradiation may cause CNHs to generate heat, leading to HA deformation and the subsequent release of MC.

As a result, MC/CNHs are predicted to exhibit a synergistic antibacterial effect between the thermal effect generated from CNHs by NIR irradiation and MC released due to heat-induced HA deformation. This result permitted the development of an innovative carbon nanomaterial, MC/HA/CNHs. These composites exhibited increased efficiency of CNHs as a carrier of MC to the affected area, improving the bactericidal effect in response to NIR irradiation and providing a photo-controlled release of the antibiotic. We propose that the NIR-light-dependent nature of the antibacterial properties of MC/HA/CNHs will allow control of localized antimicrobial activity and provide a promising strategy to address peri-implantitis.

Results and discussion

Preparation and characterization of MC/HA/CNH composites

In the present study, HA-coated CNHs (HA/CNHs) were formulated (Fig. 1A) to improve the dispersibility of CNHs in aqueous suspension and to provide the desired ability to hold and release a drug, as is expected for HA[36]. We prepared three types of CNHs from as-prepared CNHS (as-CNHs, i.e., not yet further modified) by subjecting the material to pretreatment at three different air-oxidation temperatures (500, 550,

and 575 °C). The resulting CNHs were designated CNH500, CNH550, and CNH575, respectively. Of the three, CNH575 demonstrated the best water dispersion, as shown by the observation that CNH575 remained stably dispersed after more than 24 h in water (Fig. 1B), a time point at which both CNH550 and CNH500 exhibited precipitation (Fig. 6). The high-temperature air-oxidation used to generate CNH575 was also expected to eliminate carbonaceous impurities that may remain in the pristine CNHs[17,19,21], which may disturb the drug-holding/releasing ability of the material. Meanwhile, we found that coating the oxidized CNHs with HA by mixing the oxidized reagent with HA in water could afford stable dispersions of CNH500, CNH550, and CNH575 (HA-CNHs) in water via the water-soluble HA moiety (Figs, 1B and 6).

We prepared composites of MC/HA/CNHs by mixing MC with the HA/CNHs (Fig. 1A), followed by a purification of the composite material away from the free MC. Previous work has shown that mild heating and cooling of HA potentiates the incorporation of a drug[36]; therefore, we prepared MC/HA/CNHs under illumination, thereby increasing the local temperature around the HA/CNHs. Although the actual local temperature increase could not be determined in the present study, it should be higher than the observed bulk temperature increase (10 °C) and lower than the decomposition temperature of MC (230 °C), as discussed in the following sections. This heating and cooling may be a reversible process permitting the release and loading of MC in equilibrium, such that HA/CNHs would bind MC at the final cooling step. Ultraviolet-visible (UV-Vis)-NIR absorption spectroscopy was used to confirm the successful conjugation of MC to HA/CNHs. The absorption spectra of MC/HA/CNH575 clearly showed broad peaks of absorbance originating from CNHs in the NIR to UV wavelengths, including the presence of a peak at 350 nm that is characteristic of MC (Fig. 2A). This result indicated that our process permitted effective capture of MC by HA/CNHs. Furthermore, the resemblance of the peak wavelength and width when comparing the pristine MC to the MC in HA/CNHs confirmed the absence of the molecular aggregation of MC on the HA/CNHs, an effect that might otherwise compromise drug activity[17].

Thermogravimetric analyses (TGAs) further confirmed the successful formation of MC/HA/CNH complexes. In this analysis, MC/HA/CNH575, which was selected as a representative sample, exhibited a peak at approximately 200 °C (Fig. 2B); in contrast, CNH575 did not show such a peak (Fig. 2C). Given that pristine MC and HA exhibited differential peaks of weight loss at approximately 230 °C (Fig. 7A), the novel peak at 200 °C was attributed to a conjugate of MC and HA, which may exhibit lower resistance to thermal degradation than either parent compound alone.

Transmission electron microscopy (TEM) was used to confirm the morphology of the samples. A characteristic dahlia-shaped structure was observed in both MC/HA/CNH575 (Fig. 1D) and CNH575 (Fig. 1C). This result indicated that the original structure of CNH575 had not been destroyed in the series of chemical treatments used to prepare MC/HA/CNH575 (Fig. 1A).

Photoresponsive DDS carrier ability of HA/CNH

The amount of MC adsorbed onto the CNHs was examined to elucidate the ability of HA/CNHs to serve as a DDS carrier. Here, HA/CNH550-based compounds were the

focus of experiments, given that HA/CNH550 possessed properties that were intermediate among HA/CNH500, HA/CNH550, and HA/CNH575. For HA/CNH550, the loaded amount of MC was estimated based on the amount of free MC lost during preparation of HA/CNH550, and the level of MC was measured by absorption spectrophotometry. As shown in Fig. 3A, the amount of MC loaded onto the structure was higher for oxidized CNH (i.e., CNH550) than for untreated CNH. In contrast, the presence or absence of HA during the process did not appear to affect the amounts of loaded MC.

The drug-release abilities of the MC/HA/CNHs were investigated by a dialysis technique, whereby the materials, which had or had not been irradiated with an NIR-light-emitting diode (LED), were dialyzed against saline (Fig. 3B). The use of an LED light source is expected to be practical for dental applications, given the small size and low weight of such devices. In comparisons among MC/as-CNH, MC/HA/as-CNH, MC/CNH550, and MC/HA/CNH550, the last material (a composite of MC with HA loaded on CNHs oxidized at 550 °C) showed the highest release capacity. Notably, MC/HA/CNH550 released greater amounts of MC than did MC/CNH550, demonstrating the role of HA in this material. Specifically, given that the loaded amounts of MC were comparable between MC/CNH550 and MC/HA/CNH550 (Fig. 3A), the higher release capacity of the latter indicated that the release of MC from CNH550 reflects the intervention of HA between MC and CNH. In practice, the amounts of MC released were lower than the amounts loaded. Given that the method for preparing the sample employed a reversible process in equilibrium for the loading and release of MC, the amount of the antibiotic actually released was expected to exceed the amount that was released and subsequently detected. We concluded that coating of the CNHs with HA was effective in increasing the drug-release ability of this material.

Notably, drug-release was boosted by irradiation of the composite with NIR-LED light. Specifically, MC release by MC/HA/CNH550 was 27.6% higher with irradiation than without (Fig. 3B). This difference presumably reflects photothermal effects of the NIR on CNHs, given that NIR irradiation has been shown to provide heating that in turn accelerates drug-release from HA[36].

The photothermal effects of CNH550, CNH575, and MC/HA/CNH575 were examined by measuring temperature increase following irradiation by NIR-LED light (Fig. 3C). After 10 min of irradiation, the temperature of these suspensions of composites increased by 10 °C or more, compared to that observed upon irradiation of an MC-only solution. While MC does not absorb NIR light (Fig. 2A), the MC-only sample did exhibit an increase in temperature. We conjecture that the solvent and the vessel absorbed light during NIR-LED exposure, causing the temperature to rise. Notably, the temperature increase exhibited by CNH575 was greater than that of CNH550, indicating that CNH575 is superior in utilizing the photothermal effect; this difference is expected to potentiate the release of drug from HA. Given this observation, further studies focused on MC/HA/CNH575.

Bacterial culture

To demonstrate the antibacterial effect of the CNH-based composites upon irradiation with NIR, *A.a.* was cultured with these materials in the presence and

absence of NIR. Since MC/HA/CNH575 exhibited the best temperature rise performance as described above, the effect of NIR irradiation of this composite on bacteria was evaluated. Specifically, the antimicrobial effect of MC/HA/CNH575 with and without NIR irradiation was compared, with MC alone at a concentration equivalent to 0.5 mg/mL of MC adsorption calculated above as MC0.5 and MC alone at a concentration equivalent to 2.5 mg/mL of MC dose amount as MC2.5. The bacteria survival was determined by quantifying the colony-forming units (CFU) and normalizing values to that obtained with the control (saline), for which survival was defined as 100% (Fig. 4A).

When the bacteria were incubated for 48 hours after 10 minutes of NIR-LED irradiation in the presence of MC/HA/CNH575, the bacterial survival rate after the addition of MC/HA/CNH575 was about 40% without NIR-LED irradiation, similar to that seen in the presence of 0.5 mg/mL MC alone (MC0.5). These results indicated that the effect of MC in MC/HA/CNH575 was the same with the same amount of MC alone (MC0.5). Remarkably, bacterial CFU were not detected after culturing in the presence of MC/HA/CNH575 with NIR-LED irradiation, and the difference in bacterial survival between NIR-irradiated and non-irradiated MC/HA/CNH cultures was statistically significant.

Transmission electron micrographs of the exposed bacteria are shown in Fig. 4, including cultured with saline (Fig. 4F) and in the presence of MC/HA/CNH575 without (Fig. 4G) and with (Fig. 4H) NIR irradiation. Compared to the unexposed *A.a.* in Fig. 4F, grown in the presence of MC/HA/CNH575 and irradiation (Fig. 4H), cells (white arrow) exhibited thinner cell walls that appeared to lack cytoplasm. In a separate control culture, bacterial cells cultured in the presence of CNH alone and subjected to NIR-LED irradiation exhibited a survival rate of approximately 1% (Fig. S3). Considered together, these results suggested that irradiation of MC/HA/CNH with NIR potentiates the antibiotic activity of this material, presumably by photothermal activation of the CNH component to enhance the HA-mediated release of the otherwise antimicrobial compound MC.

We extended this analysis by assessing the persistence of drug effects following dialysis of the materials. Specifically, the sample suspensions were subjected to a 48-h dialysis before adding the dialyzed composites back to cultures of bacteria (Fig. 4B). Under these conditions, *A.a,* cultures grown in the presence of 2.5 mg/mL MC alone (MC2.5) exhibited a 88% bacterial survival rate. In contrast, no bacterial CFU were detected after NIR irradiation and culture in the presence of MC/HA/CNH575 dialysed samples for 48 hours, which was significantly different from the cell viability of MC2.5. These results confirmed that CNHs serve as DDS carriers and retain the potential for photothermal activation even after a 48-h dialysis.

Gingival fluid flows at approximately 20 μL per hour[37], meaning that the typical pocket volume of 0.5 μL would be replaced some 40 times per hour[38]. Given this flow rate, the advantages and disadvantages of MC in treating bone defects may be limited to the first day of dosing[39]. In addition, to prevent the development of resistant bacteria, the use of this antibiotic should be limited to the minimum amount necessary for treatment. In fact, it has been reported that peri-implantitis patients treated with MC alone frequently yield submucosal bacterial pathogens with *in vitro* resistance to therapeutic

concentrations of doxycycline[40]. Therefore, it would be advantageous to obtain longer-term effects with a small doses of antimicrobial agents, as may be possible with the materials characterized in the present work.

Cell Culture

The use of MC/HA/CNHs for local delivery of drugs to treat peri-implant inflammation also would require that MC/HA/CNHs do not adversely affect normal cells around them. To verify the cytocompatibility of these composites, we assessed the viability of fibroblast cells (NIH/3T3) and osteoblastic cells (MC3T3-E1) in the presence of MC/HA/CNH575 and irradiated by the NIR-LED light. We first confirmed that the cells were not adversely affected by the temperature increase caused by the NIR irradiation (Fig. 9). Following exposure to the CNHs and NIR irradiation, the cells were cultured for another 48 h, and viability was assessed by measuring the cultures' DNA content using Picogreen, a fluorescent dye that stains double-stranded DNA. No statistically significant change in fibroblast cell viability was observed in cells exposed to CNHs and NIR (compared to control cultures) (Fig. 5A). However, the DNA content in the exposed samples was nominally lower for cells exposed to MC alone compared to the CTRL (saline-exposed) culture. These results are consistent with a literature report indicating that high concentrations of MC hydrochloride (exceeding 49.4 μg/mL, or 100 μM) are associated with a dose-dependent decrease in cellular differentiation and protein expression[41]. Nonetheless, we infer that exposure to MC/HA/CNH575, even with photothermal activation of the material, has minimal effects on the proliferation of fibroblast cells. In contrast, the DNA content of osteoblasts grown in the presence of MC/HA/CNH was decreased compared to that of control cultures. However, the DNA content of MC/HA/CNH-exposed osteoblasts was statistically significantly higher than that of cultures exposed to MC alone. In vitro exposure of osteoblasts to MC alone (at concentrations of 0.05 mg/mL) has been reported to be cytotoxic[41], resulting in a mean cell survival rate of 74%. Those data are consistent with the results of the present study (Fig. 5B). Nevertheless, the cytotoxic effect of MC/HA/CNHs was less than that seen with MC alone. We propose that the incorporation of MC/HA/CNHs into the microstructure of the implant surface may provide long-term efficacy against peri-implantitis, although long-term cytotoxic effects will need to be further investigated.

The most notable aspect of MC/HA/CNHs was the remarkable enhancement of antibiotic activity under NIR irradiation. This feature is expected to improve the efficacy of antimicrobial agents[42,43]. In the cases of peri-implant mucositis, it may be possible to prevent progression to peri-implantitis by using lower doses of antimicrobial agents. Treatment might consist of peeling back the mucosal tissue affected by peri-implantitis to expose the implant surface; this surface then would be thoroughly cleaned, at which point MC/HA/CNHs would be applied to the exposed surface. Subsequently, at 24-48 h after the surgery, the mucosa around the implants would be irradiated with NIR light to activate the therapeutic effect. Such an approach would not only permit the use of lower doses of antibacterial agents, but also could achieve a longer, more potent antibacterial effect.

Conclusions

In the present study, we developed MC/HA/CNH composites for use as an NIR-boosted DDS for the treatment of peri-implantitis and confirmed the material's strong antibacterial effect *in vitro*. We postulate that the use of such composites would decrease the use of MC, thereby minimizing problems related to allergies and drug resistance. MC/HA/CNHs therefore are expected to decrease the burden on the patient while providing more-effective treatment for peri-implantitis. This strategy is expected to advance the treatment of peri-implantitis by addressing the limitations of current approaches, providing a minimally invasive and effective solution for managing this common complication in implant dentistry. We propose that NIR-boosted treatment of peri-implantitis with MC/HA/CNHs, in combination with surgical procedures, will permit the targeting of relatively deep affected areas in a timely and efficacious manner.

Declaration of competing interest

The authors declare that they have no known competing financial interests or personal relationships that could have appeared to influence the work reported in this paper.

Acknowledgments

This study was reproduced from Ref. (https://doi.org/10.1039/D4NR01036A) with permission from the Royal Society of Chemistry.

This study was supported by JSPS KAKENHI (ID No. 23K09266 and Kao Crescent award to E.H., 21H01753 to Y.T., 22K19609 and 24K12996 to A.Y.), and JSPS Cooperative Research Program of "NJRC Mater. & Dev.".

The authors thank FORTE Science Communications (https://www.forte-science.co.jp/) for English language editing.

Materials & Methods

General

Minocycline hydrochloride (MC) and solvents were purchased from Fuji Film Wako Corporation (Osaka, Japan). Medium-molecular-weight hyaluronic acid (MMW-HA, 75-350 kD; GLR004) was obtained from R&D Systems (Minneapolis, MN, USA). To produce CNHs, a pure graphite target was placed in an Ar environment under conditions of room temperature and 760 Torr, and subjected to ablation using a CO_2 laser (wavelength 10.6 μm, maximum power 5 kW, pulse duration variable from 10 ms to continuous illumination, and beam diameter 10 mm).[44,45,46] A previous study has shown that the resulting CNHs were approximately 95% pure, with the majority of the

impurities consisting of graphitic spheres.[19] No metal catalyst was used in the preparation of these samples. Air-oxidized CNHs were prepared as reported previously[21]. Briefly, the CNHs placed under a flow of atmospheric air were heated by subjecting the material to progressively increasing temperature at a rate of 1.0 °C/min until a final temperature of 575 °C was achieved; the CNHs then were cooled to room temperature under a flow of atmospheric air.

Preparation of MC/CNH composites

A stock solution of 5.0 mg/mL MC was prepared by dissolving MC solid in deionized water. A solution of 1.0 mg/mL HA was prepared by dissolving HA solid in deionized water and heating the mixture at 80 °C for 60 min. Dispersions of 1.0-mg/mL CNHs were formulated by disperding CNHs [consisting of as-prepared CNHs (as-CNHs, i.e., not yet further modified), CNHs oxidized at 550 °C (CNH550), or CNHs oxidized at 575 °C (CNH575)] in deionized water.

HA/CNH composites were prepared by adding 0.10 mL of HA solution (0.10 mg) to 1.0 mL of the dispersion of CNHs (1.0 mg); the resulting mixture was irradiated using an LED light (738 nm, 200 mW/cm^2, 20 °C) while shaking for 30 min. The irradiated mixture then was centrifuged (10,000 *g*, 10 min, 20 °C) to pellet the composites.

MC/HA/CNH composites were prepared by adding 1.0 mL of MC solution (5.0 mg) to 1.0 mL (1.0 mg) of HA/CNH composite. The resulting mixture was irradiated (as above) for 10 min while shaking at room temperature, and the irradiated mixture then was centrifuged (as above) to pellet the composites. The resulting MC/HA/CNHs were suspended in saline (9.0 g/L NaCl, pH=4.5–8.0, Otsuka Normal Saline Otsuka Pharmaceutical Factory, Inc., Tokushima, Japan) for use in the bacterial or cell culture experiments. The MC/HA/CNH samples were observed using transmission electron microscopy (TEM; JEM1400, JEOL, Tokyo, Japan), conducted at an acceleration voltage of 80 V.

Absorption spectroscopy

To estimate the dispersion of the MC/HA/CNH samples, the absorbance of the CNH and MC/HA/CNH suspensions were determined at 350 nm using a Nanodrop UV-Vis spectrophotometer (Thermo™ INSIGHT, Thermo Fisher Scientific, Waltham, MA, USA).

Thermogravimetric analysis

Prior to thermogravimetric analysis (TGA), the MC/HA/CNH dispersions were lyophilized using a VD-400 F instrument (TAITEC, Koshigaya, Japan) to obtain black powders. TGA was performed with a TG 8120 instrument (Rigaku Corporation, Tokyo, Japan). In each trial, a 2.0-mg sample was placed on a platinum pan and the sample temperature was increased from ambient to 900 °C at a rate of 10 °C/min while the sample was maintained under a 100-mL/min flow of N_2.

Quantification of released MC

The amount of MC released from each MC/HA/CNH specimen was calculated by measuring the weight of the supernatant obtained by centrifugation during the

MC/HA/CNH sample preparation process and the absorbance at 350 nm (using the UV-Vis spectrophotometer, as described above). The quantity of MC released from the MC/HA/CNH sample was determined as follows: the MC/HA/CNH dispersion was added to the insert dish (Nunc™ Polycarbonate Cell Culture Inserts in Multi-Well Plates; pore size, 0.4 μm), and the dish was exposed to light while shaking for 10 min using Analog Shaker Seesaw (SK-R1807-E, DLAB, Beijing, China). The absorbance of the solution outside the insert then was measured.

Measurement of photothermal effect

To investigate the photothermal effect on MC/HA/CNH, a temperature-rise experiment was conducted as follows: samples (180 μL) were placed in a 96-well plate (Tissue culture plate, Flat Bottom with Low Evaporation, Polystyrene, 353075, FALCON, Corning, NY, USA) at room temperature, and the plate was subjected to NIR light irradiation (738 nm, 400 mW/cm^2) for 10 min. During the irradiation interval, the temperatures of the samples were measured every 20 seconds using thermometer (TX10-01, Yokogawa M&C Corporation, Tokyo, Japan).

Bacterial culture

For bacterial culture, MC/HA/CNH575 was used because it exhibited the best temperature rise performance. To evaluate the effect of this composite on bacteria, bacteria activity was compared with MC alone at a concentration equivalent to 0.5 mg/mL of MC adsorption calculated above (MC0.5) and MC alone at a concentration equivalent to 2.5 mg/mL of MC dose amount (MC2.5).

To assess the persistence of drug effects, we performed dialysis on three materials: MC0.5, MC2.5 and a MC/HA/CNH575 sample. For each trial, an aliquot of the sample (0.3 mL of the MC solutions or 0.5 mL of the MC/HA/CNH575 suspension) was transferred to a Slide-A-Lyzer, (molecular weight cutoff, 2 kD; volume range 0.2-0.5 mL; Thermo Fisher) dialysis cassette, and the cassette then was placed in 10 mL of saline at room temperature. At 48 h, an aliquot (180 μL) of the dialyzed sample was recovered from within the cassette.

A stock suspension of MC/HA/CNHs was prepared by dispersing the composite at 1.0 mg/mL in saline. Aliquots (180 μL) of the MC/HA/CNH suspension were combined with 20 μL of bacterial suspensions of *Aggregatibacter actinomycetemcomitans* (*A.a.*: ATCC 29522) to a final density of 2.0×10^4 cell-forming units (CFU) per mL. The bacteria were incubated for 10 min with NIR-LED irradiation using an NIR-LED light (738 nm, 400 mW/cm^2) in the presence of MC/HA/CNH575. The bacteria were also incubated in the presence of MC0.5, MC2.5, and MC/HA/CNH575 without irradiation of NIR-LED light for 10 min.

Ten minutes after seeding, the bacterial suspensions were diluted 10-fold in brain-heart infusion (BHI) broth (BHIB; Becton Dickinson, Franklin Lakes, NJ, USA), and an aliquot (100 μL) of the dilution was spread on BHI agar (Becton Dickinson). The resulting plates were incubated at 37 °C under microaerophilic conditions in a candle jar for 48 h. Colony counts (CFU) then were determined using Image J Fiji[47] and used to calculate the cell density of the exposed cultures.

TEM observations of bacteria

The bacteria were fixed with 2% glutaraldehyde, stained with 1% OsO_4, dehydrated, and embedded in epoxy resin. The resulting blocks were subjected to ultrathin (approximately 80 nm thickness) sectioning using an ultramicrotome (Leica, Wetzlar, Germany) with a diamond knife (DiATOME, Nidau, Switzerland), and the sections were examined by TEM (JEM1400, JEOL, Tokyo, Japan) at 80 V acceleration.

Cell culture

Two cell lines were used to determine cytotoxicity: NIH/3T3, a mouse embryonic fibroblasts cell line[48,49]; and MC3T3-E1, a mouse calvaria osteoblastic cell line[50,51]. All cell culture was conducted at 37 °C in a 5% CO2 environment. NIH/3T3 cells were seeded in 96-well plates (IWAKI, AGC Techno Glass, Shizuoka, Japan) at 1×10^4 cells/well and cultured in Dulbecco's Modified Eagle's Medium-(DMEM) high glucose (Sigma-Aldrich, St. Louis, MO, USA) containing 10% fetal calf serum (FCS; Funakoshi, Tokyo, Japan) and 1x penicillin/streptomycin (corresponding to 50 U/mL penicillin and 50 mg/mL streptomycin; Thermo Fisher Scientific/Gibco, Waltham, MA, USA). MC3T3-E1 cells were cultured in Eagle's Minimum Essential Medium (MEM; Sigma-Aldrich) containing 10% fetal bovine serum (FBS; CELLECT, France), 2 mM glutamine, and 1x penicillin/ streptomycin. At 5 h after seeding, the medium was replaced by the respective medium containing the dispersion of MC/HA/CNHs at 180 µL/well. For controls, the medium instead was replaced with the respective medium supplemented with MC or CNHs at 1.0 mg/mL. Following the replacement of the medium, the wells were illuminated for 30 min using the NIR-LED. Following irradiation, the plates were cultured for another 24 h.

Quantification of DNA content

Following the 24 h of culturing, the DNA content of each sample was determined, as follows. The cells of each well were washed once with phosphate-buffered saline (pH 7.4; PBS) and the resulting cell pellets were resuspended in 50 µL/well of a suspension composed of 0.2% IGEPAL CA630 (octylphenoxy poly(ethyleneoxy)ethanol, branched; a non-ionic, non-denaturing detergent; Sigma-Aldrich), 10 mM Tris-HCl (pH 7.4), and 1 mM $MgCl_2$. The samples were frozen, thawed, and homogenized. Next, a solution of 4 M NaCl and 0.1 M phosphate buffer (pH 7.4) was dispensed into the plate at 50 µL/well (to lyse the cells), and the well contents were mixed and then centrifuged. An aliquot (80 µL/well) of the resulting DNA-containing supernatant was transferred to a 96-well black, flat-bottom plate, and an equal volume of the DNA dye PicoGreen (Molecular Probes/Thermo Fisher) (diluted 200-fold in TE buffer (10 mM Tris-HCl, 1 mM ethylenediamine tetraacetic acid (EDTA), pH7.4)) was dispensed into each well. Following mixing, the light emission from each well was measured using a microplate reader (infinite F200 PRO; TECAN, Männedorf, Swizerland) at excitation/emission wavelengths of 365/450 nm (respectively). Emission levels were converted to DNA concentrations by comparison to a standard curve generated using a serial dilution of a DNA of known concentration.

Statistical analysis

CFU values were analyzed by two-tailed one-way ANOVA with post hoc uncorrected Dunn's tests. For the bacteria culture, the data represent three biological replicates. DNA content was analyzed by two-tailed one-way ANOVA with post hoc Holm-Sidak's multiple comparisons tests. Statistical analyses were conducted using GraphPad Prism 7 (GraphPad Software, Boston, MA, USA). P <0.05 was considered statistically significant.

Figures

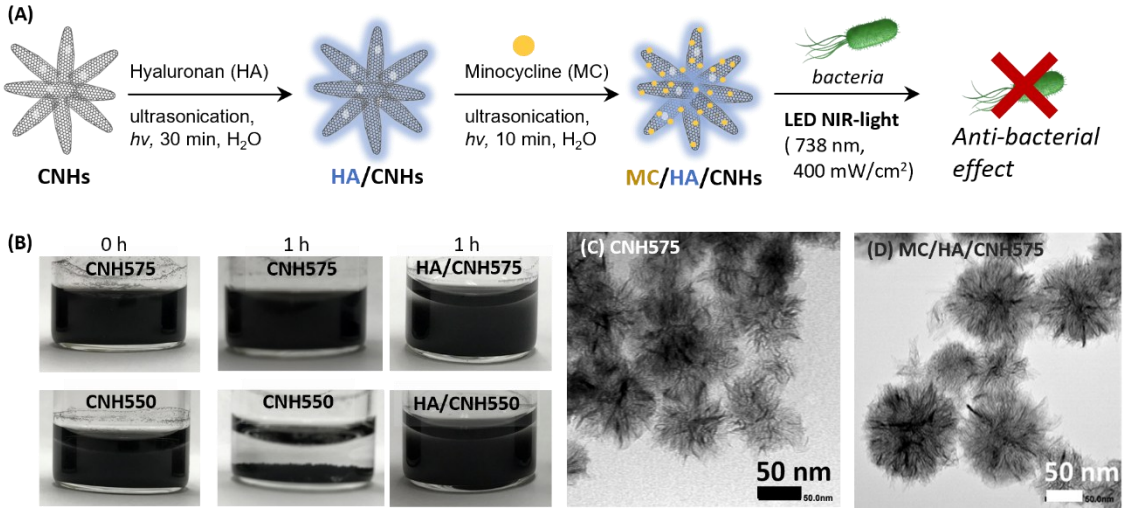

Fig. 1. (A) Scheme for synthesis of the composite of minocycline/hyaluronan/CNHs (MC/HA/CNHs), and for assessment of NIR-light-induced antibacterial effects. (B) Photographs of suspensions of CNH575, CNH550 (carbon nanohorns oxidized at 575, and 550 °C, respectively), HA/CNH575, and HA/CNH550 acquired at 0 and 1 h after dispersion by sonication. TEM images of (C) CNH575 and (D) MC/HA/CNH575.

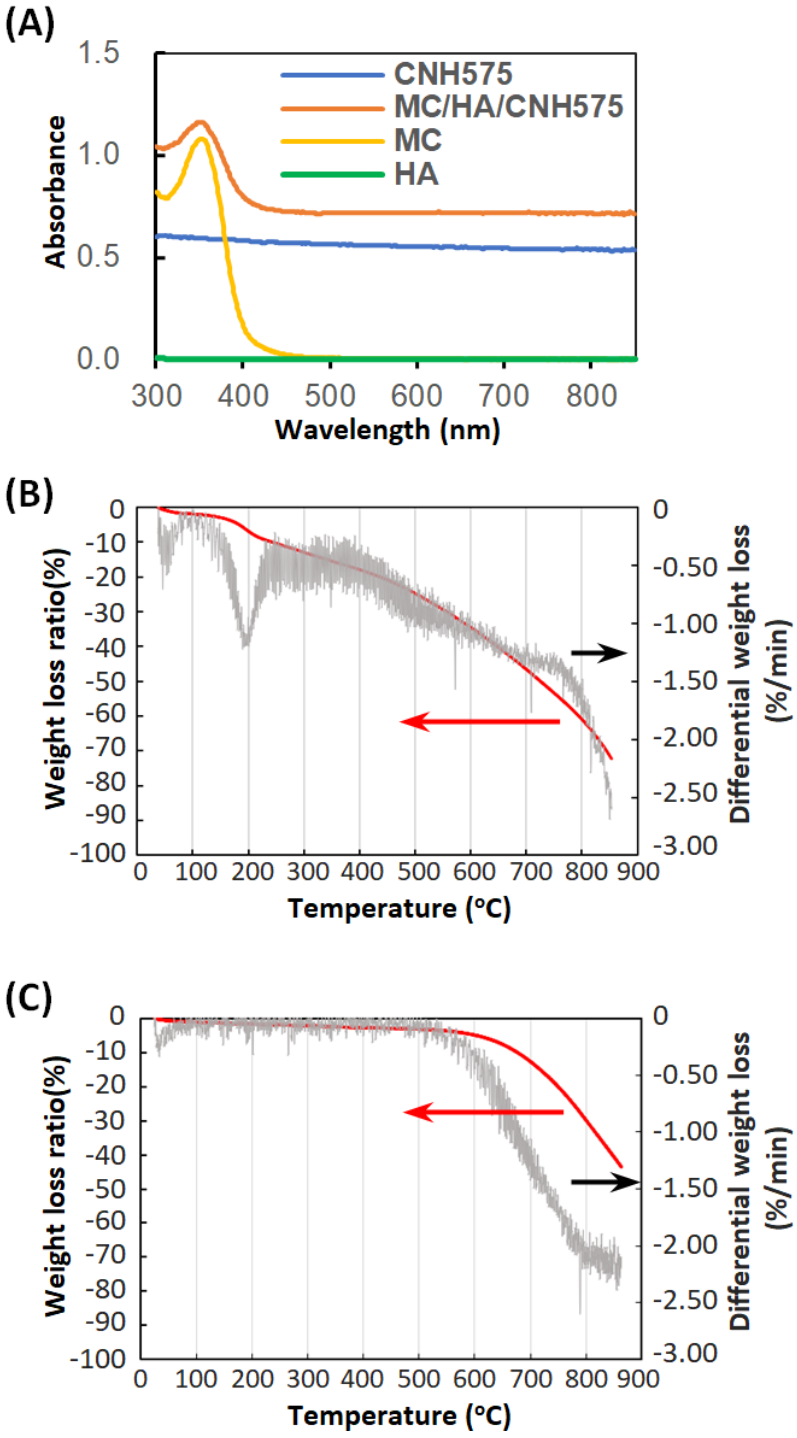

Fig. 2. (A) Absorbance spectra of MC (62.5 μg/mL; yellow line), HA (1.0 mg/mL; green line), CNH575 (100 μg/mL; blue line), and MC/HA/CNH575 (100 μg/mL; orange line) dispersed in water. Thermogravimetric weight loss (red lines) and differential weight loss (gray lines) data were obtained for (B) MC/HA/CNH575 and (C) CNH575 maintained under an N_2 flow.

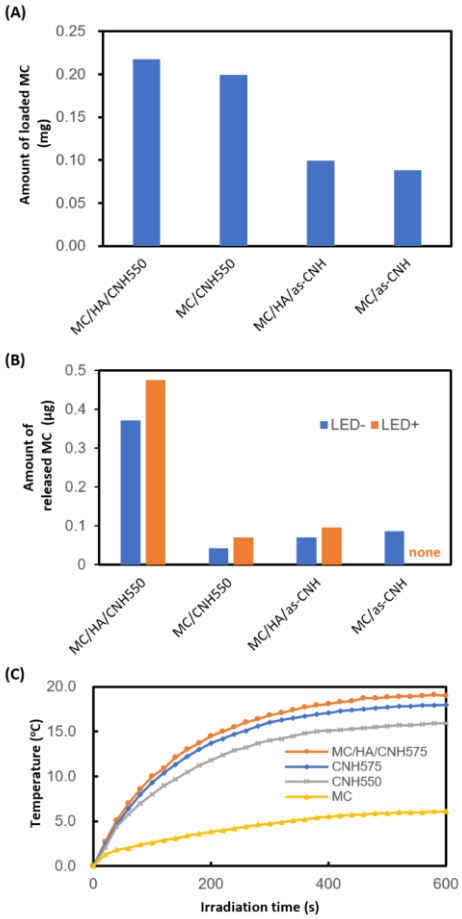

Fig. 3. (A) Amount of minocycline (MC) loaded on CNH550 (CNHs oxidized at 550 °C), hyaluronan (HA)/CNH550, as-CNH [as-prepared CNHs (i.e., not yet further modified)), and HA/as-CNH (using CNHs suspended at 1.0 mg/mL in 1.0 mL saline). (B) Amount of MC released from MC/CNH550 or MC/HA/CNH550 (using CNHs suspended at 1.0 mg/mL in 0.3 μL saline) and then passed through a 0.4-μm-filter (Nunc™ Polycarbonate Cell Culture Inserts in Multi-Well Plates; pore size, 0.4 μm). NIR-LED irradiation: 738 nm, 200 mW/cm^2, 0.8-cm beam diameter, 10 min). "none" indicates the value below the detection limit. (C) Temperature of suspensions of the specimens subjected to the LED irradiation.

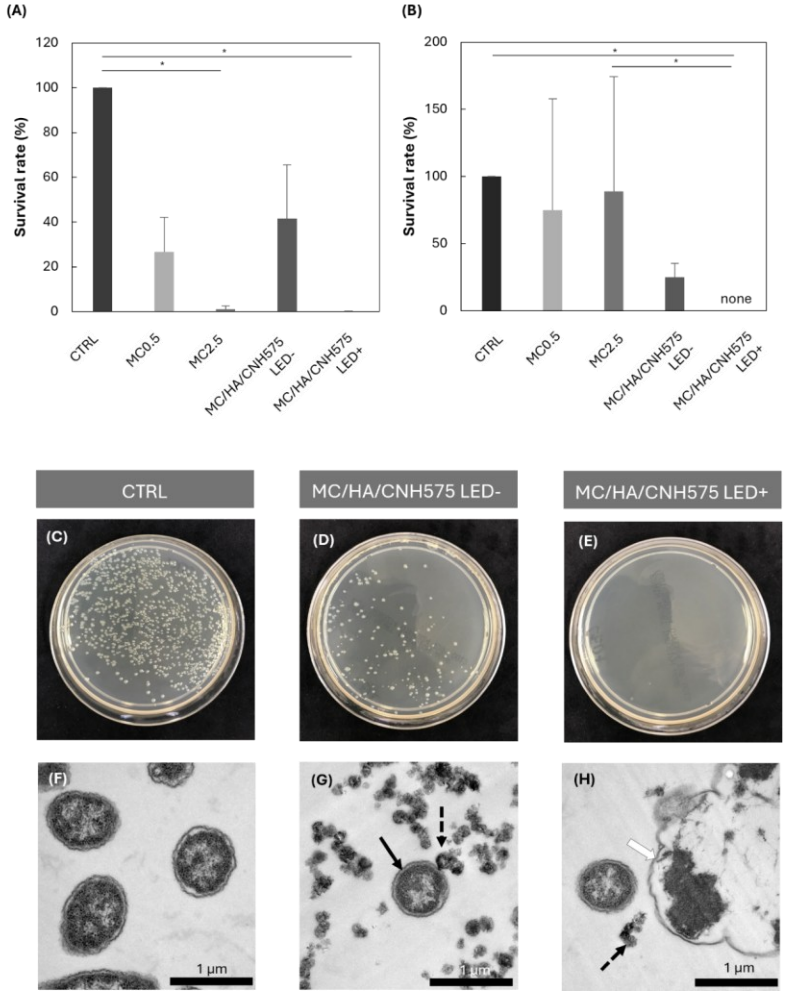

Fig. 4.(A) Survival of *Aggregatibacter actinomycetemcomitans* (*A.a.).* The plating on agar culture was conducted prior to incubation with saline (Control; CTRL), minocycline (MC), and MC/HA/CNH575. Light-emitting diode (LED) irradiation: 738 nm, 400 mW/cm^2, 10 min. Pre-dialysis samples were used. (B) Samples 48 h after dialysis. Images of the agar plates with *A.a.* bacteria (C) cultured under the control conditions, (D) cultured with MC/HA/CNH575_LED-, and (E) cultured with MC/HA/CNH575_LED+. Transmission electron microscopy (TEM) images of *A.a.* bacteria (F) cultured under the control conditions, (G) cultured with MC/HA/CNH575_LED-, and (H) cultured with MC/HA/CNH575_LED+. *A.a.* bacteria (solid arrow) and MC/CNH (dashed arrow) were observed in (D). Dead bacteria (white arrow) were observed in (E). Initial *A.a.* cell density: 2.0 × 10^4 Colony-forming units (CFU)/mL. LED irradiation was conducted for 10 min at 738 nm, 400 mW/cm^2. CTRL: saline (control). MC0.5 and MC2.5 correspond to solutions containing MC at 0.5 and 2.5 mg/mL (respectively). MC concentration in MC/HA/CNH575 suspension was 0.697 mg/mL. Data are presented as mean + SD (n = 3). Values were analyzed by two-tailed one-way ANOVA with post hoc uncorrected Dunn's tests (*P < 0.05, **P < 0.01,***P < 0.001).

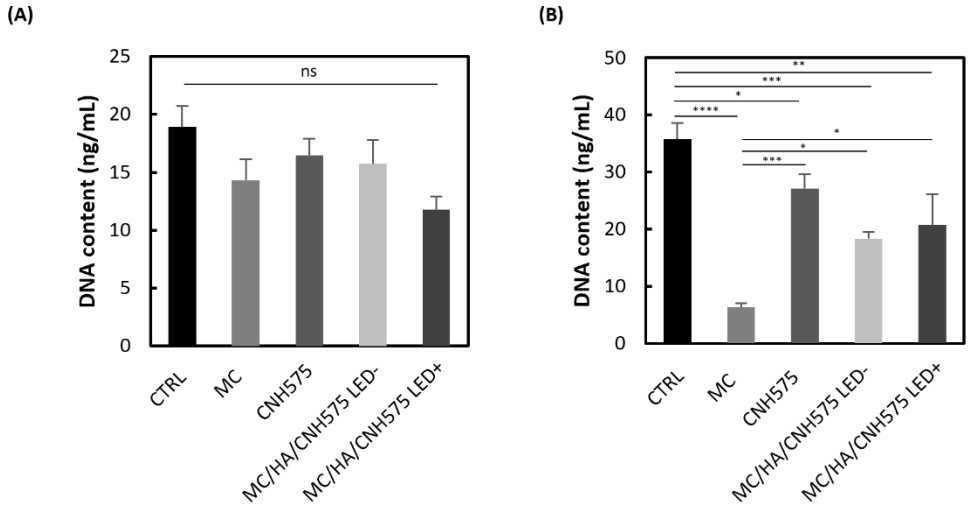

Fig. 5. Cell viability as assessed by DNA content of (A) NIH/3T3 and (B) MC3T3-E1 cells. "LED+" cultures were subjected to irradiation with an NIR-LED light (738 nm, 200 mW/cm^2, 30 min). "LED-" cultures were left in the dark for the equivalent duration. MC concentrations in the MC/HA/CNH575 composite in the culture media used for NIH/3T3 and MC3T3-E1 cells were 0.88 and 0.80 mg/mL, respectively. (n = 4, ns, not significant, *P < 0.05, **P < 0.01, ***P < 0.001, **** P < 0.0001).

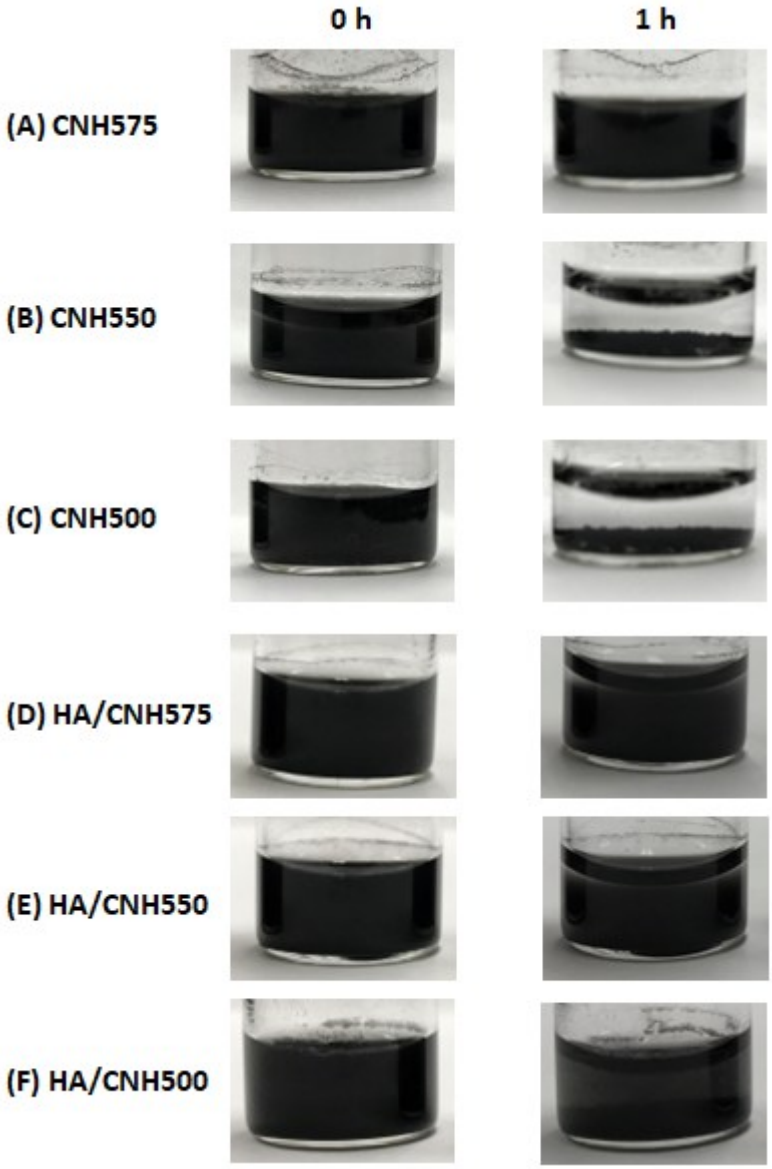

Fig. 6. Photographic images of suspensions of (A) CNH575, (B) CNH550, (C) CNH500 (carbon nanohorns oxidized at 575, 550, and 500 °C, respectively), (D) HA/CNH575, (E) HA/CNH550, and (F) HA/CNH500 specimens (hyaluronan coated CNH575, CNH550, and CNH500, respectively) at 0 and 1 h after dispersion.

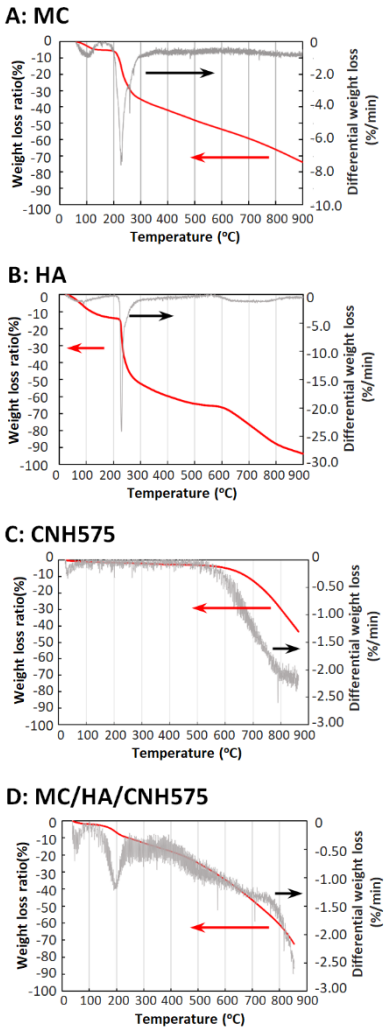

Fig. 7. Thermogravimetric (TG; red lines) and differential TG (DTG; gray lines) data were obtained for (A) MC alone, (B) HA, (C) CNH575, and (D) MC/HA/CNH575 specimens. Temperatures were increased at a rate of 10 °C/min for samples maintained under a 100 mL/min flow of N_2.

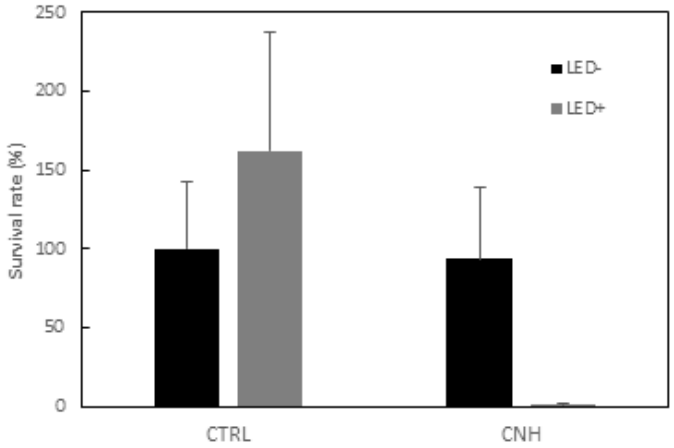

Fig. 8. Survival rates of *Aggregatibacter actinomycetemcomitans* (*A.a.*; initial density, 2.0×10^4 CFU/mL) following exposure to CNH575 (CNH) or saline (Control; CTRL) followed by irradiation (LED+; black bars) or lack thereof (LED-; gray bars) with an NIR-LED (738 nm, 400 mW/cm^2) for 10 min. Exposure and irradiation were performed on bacterial suspensions, which then were plated on growth agar and incubated at 37 °C for 48 h before counting of colonies. Data are presented as mean + SD (n = 3).

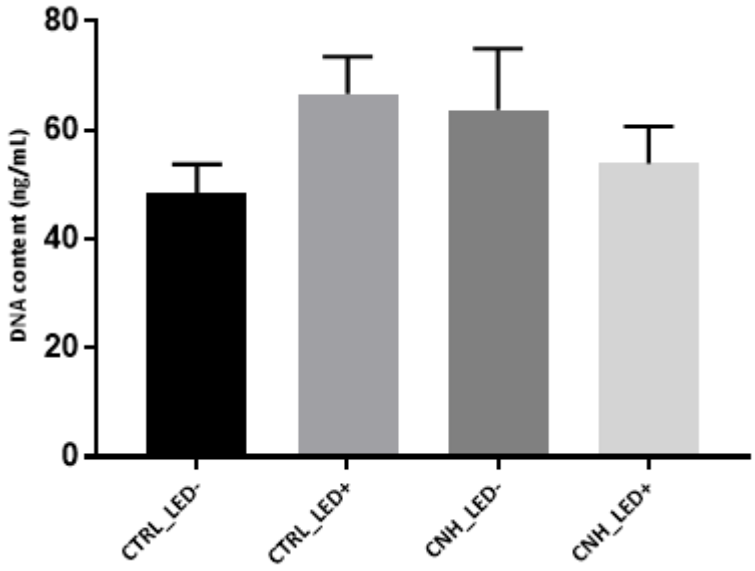

Fig. 9. Cell viability as assessed by DNA content of NIH/3T3 cells. Carbon nanohorns (CNH, 0.01 mg/mL) were added to the "CNH" cultures. "LED+" cultures were subjected to irradiation with an NIR-LED light (738 nm, 400 mW/cm^2, 10 min). "LED-" cultures were left in the dark for the equivalent interval. Data are presented as mean + SD (n = 4).

References

1 K. El Kholy, D. Buser, J.-G. Wittneben, D. D. Bosshardt, T. E. Van Dyke and M. J. Kowolik, *Materials (Basel).*, 2020, **13**, 3421.

2 D. Buser, S. F. M. Janner, J. Wittneben, U. Brägger, C. A. Ramseier and G. E. Salvi, *Clin. Implant Dent. Relat. Res.*, 2012, **14**, 839–851.

3 R. Guarnieri, R. Reda, D. Di Nardo, F. Pagnoni, A. Zanza and L. Testarelli, *J. Pers. Med.*, 2024, **14**, 342.

4 A. Rokn, H. Aslroosta, S. Akbari, H. Najafi, F. Zayeri and K. Hashemi, *Clin. Oral Implants Res.*, 2017, **28**, 314–319.

5 F. Schwarz, J. Derks, A. Monje and H. Wang, *J. Clin. Periodontol.*, 2018, **45**, S246–S266.

6 L. J. Tavares, A. C. Pavarina, C. E. Vergani and E. D. de Avila, *Photodiagnosis Photodyn. Ther.*, 2017, **17**, 236–244.

7 A. Roccuzzo, A. Stähli, A. Monje, A. Sculean and G. Salvi, *J. Clin. Med.*, 2021, **10**, 1107.

8 P. Sahrmann, F. Gilli, D. B. Wiedemeier, T. Attin, P. R. Schmidlin and L. Karygianni, *Microorganisms*, 2020, **8**, 661.

9 Å. Leonhardt, B. Adolfsson, U. Lekholm, M. Wikström and G. Dahlén, *Clin. Oral Implants Res.*, 1993, **4**, 113–120.

10 D. Herrera, T. Berglundh, F. Schwarz, I. Chapple, S. Jepsen, A. Sculean, M. Kebschull, P. N. Papapanou, M. S. Tonetti and M. Sanz, *J. Clin. Periodontol.*, 2023, **50**, 4–76.

11 R. Junker, A. Dimakis, M. Thoneick and J. A. Jansen, *Clin. Oral Implants Res.*, 2009, **20**, 185–206.

12 A. Liñares, I. Sanz-Sánchez, J. Dopico, A. Molina, J. Blanco and E. Montero, *J. Clin. Periodontol.*, 2023, **50**, 224–243.

13 G. Baima, F. Citterio, M. Romandini, F. Romano, G. M. Mariani, N. Buduneli and M. Aimetti, *Clin. Oral Implants Res.*, 2022, **33**, 1069–1086.

14 Y. C. M. De Waal, | Lewis Winning, | Andreas Stavropoulos and I. Polyzois, *J Clin Periodontol*, 2022, 1–12.

15 T. Larsen and N.-E. Fiehn, *J. Clin. Periodontol.*, 1997, **24**, 254–259.

16 K. G. Blumenthal, J. G. Peter, J. A. Trubiano and E. J. Phillips, *Lancet*, 2019, **393**, 183–198.

17 N. C. Maiti, S. Mazumdar and N. Periasamy, *J. Phys. Chem. B*, 1998, **102**, 1528–1538.

18 J. Ackermann, J. T. Metternich, S. Herbertz and S. Kruss, *Angew. Chem. Int. Ed. Engl.*, 2022, **61**, e202112372.

19 J. Fan, M. Yudasaka, D. Kasuya, T. Azami, R. Yuge, H. Imai, Y. Kubo and S. Iijima, *J. Phys. Chem. B*, 2005, **109**, 10756–10759.

20 G. D. Goaslind, P. B. Robertson, C. J. Mahan, W. W. Morrison and J. V. Olson, *J. Periodontol.*, 1977, **48**, 768–771.

21 J. Fan, M. Yudasaka, J. Miyawaki, K. Ajima, K. Murata and S. Iijima, *J. Phys. Chem. B*, 2006, **110**, 1587–1591.
22 S. Zheng, Y. Tian, J. Ouyang, Y. Shen, X. Wang and J. Luan, *Front. Chem.*, 2022, **10**, 990362.
23 K. AbouAitah, F. Sabbagh and B. S. Kim, *Nanomaterials*, 2023, **13**, 2666.
24 S. Iijima, M. Yudasaka, R. Yamada, S. Bandow, K. Suenaga, F. Kokai and K. Takahashi, *Chem. Phys. Lett.*, 1999, **309**, 165–170.
25 J. Miyawaki, M. Yudasaka, T. Azami, Y. Kubo and S. Iijima, *ACS Nano*, 2008, **2**, 213–26.
26 T. Sari, H. Eri, S. Masatoshi, M. Eijiro, T. Yuta, U. Natsumi, Y. Masako, I. Sumio and Y. Atsuro, *Artif. Cells, Nanomedicine, Biotechnol.*, 2021, **0**, 1–18.
27 E. Hirata, E. Miyako, N. Hanagata, N. Ushijima, N. Sakaguchi, J. Russier, M. Yudasaka, S. Iijima, A. Bianco and A. Yokoyama, *Nanoscale*, 2016, **8**, 14514–14522.
28 C. Stangel, A. Kagkoura, N. Pippa, D. Stellas, M. Zhang, T. Okazaki, C. Demetzos and N. Tagmatarchis, *Nanoscale Adv.*, 2023, **5**, 6847–6857.
29 M. Zhang, T. Okazaki, Y. Iizumi, E. Miyako, R. Yuge, S. Bandow, S. Iijima and M. Yudasaka, *J. Mater. Chem. B*, 2016, **4**, 121–127.
30 S. M. Hosseini, J. Mohammadnejad, R. Najafi-Taher, Z. B. Zadeh, M. Tanhaei and S. Ramakrishna, *ACS Appl. Bio Mater.*, 2023, **6**, 1323–1338.
31 J. K. Cha, J. S. Lee and C. S. Kim, *J. Dent. Res.*, 2019, **98**, 288–295.
32 S. Javed and K. Kohli, *Curr. Drug Deliv.*, 2010, **7**, 398–406.
33 Y. Maeda, E. Hirata, Y. Takano, N. Sakaguchi, N. Ushijima, A. Saeki, S. Kimura, K. ichiro Shibata, M. Yudasaka and A. Yokoyama, *Carbon N. Y.*, 2020, **166**, 36–45.
34 P. Zhang, Q. Wu, J. Yang, M. Hou, B. Zheng, J. Xu, Y. Chai, L. Xiong and C. Zhang, *Acta Biomater.*, 2022, **146**, 450–464.
35 C. Gao, J. Jian, Z. Lin, Y.-X. Yu, B.-P. Jiang, H. Chen and X.-C. Shen, *Langmuir*, 2019, **35**, 8228–8237.
36 X. Hou, D. Zhong, H. Chen, Z. Gu, Q. Gong, X. Ma, H. Zhang, H. Zhu and K. Luo, *Carbohydr. Polym.*, 2022, **292**, 119662.
37 H. Makkar, Y. Zhou, K. S. Tan, C. T. Lim and G. Sriram, *Adv. Healthc. Mater.*, 2023, **12**, 2202376.
38 J. M. Goodson, in *Journal of Dental Research*, 1989, vol. 68, pp. 1625–1632.
39 H. Lu and C. Chei, *J. Periodontal Res.*, 2005, **40**, 20–27.
40 T. E. Rams, J. E. Degener and A. J. Van Winkelhoff, *Clin. Oral Implants Res.*, 2014, **25**, 82–90.
41 J. B. Park, *J. Craniofac. Surg.*, 2011, **22**, 1839–1842.
42 H. K. Lu and C. J. Chei, *J. Periodontal Res.*, 2005, **40**, 20–27.
43 J. Zhao, Y. Wei, J. Xiong, H. Liu, G. Lv, J. Zhao, H. He, J. Gou, T. Yin, X. Tang and Y. Zhang, *Int. J. Pharm.*, 2023, **636**, 122802.
44 T. Azami, D. Kasuya, R. Yuge, M. Yudasaka, S. Iijima, T. Yoshitake and Y. Kubo, *J. Phys. Chem. C*, 2008, **112**, 1330–1334.
45 R. Yuge, F. Nihey, K. Toyama and M. Yudasaka, *Carbon*, 2018, **138**, 379–383.

46 S. Iijima, M. Yudasaka, R. Yamada, S. Bandow, K. Suenaga, F. Kokai and K. Takahashi, *Chem. Phys. Lett.*, 1999, **309**, 165–170.
47 J. Schindelin, I. Arganda-Carreras, E. Frise, V. Kaynig, M. Longair, T. Pietzsch, S. Preibisch, C. Rueden, S. Saalfeld, B. Schmid, J. Y. Tinevez, D. J. White, V. Hartenstein, K. Eliceiri, P. Tomancak and A. Cardona, *Nat. Methods*, 2012, **9**, 676–682.
48 G. J. Todaro and H. Green, *J. Cell Biol.*, 1963, **17**, 299–313.
49 E. Miyako, T. Deguchi, Y. Nakajima, M. Yudasaka, Y. Hagihara, M. Horie, M. Shichiri, Y. Higuchi, F. Yamashita, M. Hashida, Y. Shigeri, Y. Yoshida and S. Iijima, *Proc. Natl. Acad. Sci. U. S. A.*, 2012, **109**, 7523–8.
50 H. Kodama, Y. Amagai, H. Sudo, S. Kasai and S. Yamamoto, *Japanese J. Oral Biol.*, 1981, **23**, 899–901.
51 K. Ueda, C. Ma, M. Izumiya, C. Kuroda, H. Ishida, T. Uemura, N. Saito, K. Aoki and H. Haniu, *Nanomater. (Basel, Switzerland)*, 2023, **13**, 244.